

A Novel Graph Convolutional Neural Network Method for Improving Phase Severance Formation Planning in Polymer Alloys

Dr. Parag Amin¹, Nagraj Patil², Dr. Vinod Mansiram Kapse³, Dr. Intekhab Alam⁴

¹Director, Department of ISME, ATLAS SkillTech University, Mumbai, Maharashtra, India, Email: parag.amin@atlasuniversity.edu.in

²Associate Professor, Department of Mechanical Engineering, Faculty of Engineering and Technology, JAIN (Deemed-to-be University), Ramanagara District, Karnataka - 562112, India, Email: nagaraj.patil@jainuniversity.ac.in

³Director, Department of Electronics and Communication Engineering, Noida Institute of Engineering and Technology, Greater Noida, Uttar Pradesh, India, Email: director@niet.co.in

⁴Assistant Professor, Maharishi School of Engineering & Technology, Maharishi University of Information Technology, Uttar Pradesh, India, Email: intekhab.pasha54@gmail.com

The use of forward analysis (FA) and inverse design (ID) procedures is crucial in several scientific and engineering fields as it facilitates the investigation, comprehension, and enhancement of intricate systems. This method is used in the domains of environmental science, engineering, and physics. Inverse design involves estimating input parameters or configuration that will achieve goals by moving backwards. This study focuses on Young's modulus (YM) as the sole property under consideration. Our suggested method Improved Gradient Graph Convolutional Neural Network (IGGCNN) works well in material design, control, and optimisation, when the objective is to identify the best solutions that satisfy certain performance requirements. This project develops a framework focused on utilizing machine learning techniques to foresee a possession based on the stage departure organization of a polymer alloy (FA), and employs ID to produce the arrangement from the needed assets. This research, sole attribute to Young's modulus. Convolutional neural networks (CNNs) are used for the FA, and random searches are used to achieve the inverse design, which is a model that combines CNNs with Graph Neural Networks (GNNs). The best qualities of several polymers with different substances to create new and improved attributes.

Keywords: Forward Analysis (FA) Inverse, Design (ID), Convolutional Neural Network (CNN), Young's Modulus (YM).

1. Introduction

The process of creating composite substances involves mixing fibres for reinforcement and matrix resins for the substrate. It is anticipated that materials made from composites would have a variety of functions that are not possible with one substance because of their low weight, outstanding durability, and high stiffness (Daru (2019)). Specifically, their superior tensile and chemical traits, carbon-fibre-reinforced polymers (CFRPs) have found widespread use. The goal of material research is to discover useful components and enhance the qualities of composites (Saeed et al (2019). Composite substances, like CFRPs, employ polymer alloys as its matrix resins since they are made of a blend of several polymers he total characteristics of those combinations are influenced by the phase segregation architecture (Shajkofci and Liebling (2019)). Micro-phase segregation frameworks, named because of the composed of ordered groupings in microscopic stage divorces which have been found to occur in polymers alloys including polymers (Tabish et al (2020)). Considering the amount of stress, it seems that the constructions' size is ideal for attaining exceptional strength. Based on their structure, polymer alloys have cubic, hexagonal, gyroid, and lamellar configurations, the chemical phase diagram for those structures is additionally known (Mann, and Kalidindi (2022)). These factors have led to increased interest in and research on polymer alloys with micro-phase segregation features as effective matrix resin for enhancing the characteristics and performance of composite components. In the process of developing new materials such as copolymer combinations with noteworthy characteristics and functions, several chemical research and strength assessments are conducted (Fakher et al (2021)). However, the time and money required for these testing and studies are quite high. A lot of computational modelling is used to lower these expenses. For instance, in the area of polymers compounds, separation of phases architectures are predicted using models that utilize consistent with fields, and the macro deformation of these structures is computed by computational modelling based on the homogenizing technique [6]. These studies allow for very accurate simulations of experiments under different settings; nevertheless, certain simulations with a large number of repeated computations have a significant processing cost. New techniques that are suitable for fast and accurate simulations are needed. There have been several efforts to search across large design parameters spaces for components or structures with the necessary qualities and functionality (Yamanaka et al (2017)). This method is known as "inverse research" or "inverse design" as it is the antithesis of forward analyses. Researchers with experience in the field have so far found a great deal of high-performing materials via a great deal of trial and error [8]. As a result, a novel approach to inverse design is needed, that proposes a synthetic procedure and a framework of the substance to be synthesized from the performance that is intended. Wang et al (2016) examined deep learning model-based framework for the ID of structure from materials using a macroscopic perspective features. In the framework, "stresses" will be taken into account as microscopic qualities and "plastic alloy's phase separation architectures" as structural features. Hiraide et al (2023) presented the comfort issue, and is dependent on the materials used in sports equipment construction. After that, it discusses composite polymers in thoroughness, provides a case study, and assesses if the supplies are appropriate for usage in sportswear. Feng and Wang (2022) assessed a number of approaches to address the challenges, including the most recent linear notation, Big SMILES, for the identification of fingerprints augmenting the dataset at hand with an

adequate approximating, utilizing a mixed-dimension opinions method, and utilizing a dualconvolutional-model framework. Yan et al (2021) which looked at a novel filler material polymer-aluminium alloy hybridization foam as a substitute for traditional closed-cell aluminium foams in slender in squared tubes constructed of aluminium alloy is presented in this publication. To create the hybrid foam-filled frameworks, latex or epoxy were injected into open-cell foam made of aluminium alloy inside of slender in tube. The production of fuel during the thermal disintegration of the layered polymers was also examined in the work. Using a gas chromatograph-mass spectrometer (GC-MC) to study the released gas, it was discovered that volatile compounds made up the majority of the mixture (Duarte et al (2019) . Hossain et al (2021) covered several energy storage processes and provides a basic understanding of how to build and develop various materials to create appropriate electrodes in the quest of a stable, high-energy efficiency super capacitor design and manufacture of various material choices for electrodes, including conducting polymers, metal oxide chlorine compounds, carbides, nitrides, and These molecules is the subsequent emphasis of the current article. Shaikh et al (2022) evaluated polymer mixes have to be compatible with certain biological applications, Compatibility has enabled a broad range of blending techniques that increase the mechanical and cellular responsiveness of polymer mixtures. Classification and comprehending the characteristics of such systems are the main goals of the next section. Zarrintaj et al (2020) one weight percent of the total weight of the fibres or 1 weight percent was placed onto the Fe fibres. Neamtu et al (2020) focussed on the latest developments of management solutions for these intrinsic problems, which can be broadly classified into three categories: friction stir-based recycling, non-weld-thinning FSW, and self-supported FSW. The article is to highlight the relevant technological advancements, process variables, mechanical characteristics, and structural attributes Meng et al (2021). Zhou et al (2022) used a combination of modelling and experimentation to examine the bending reaction of a new magnesium alloy facesheet and 3D-printed polylactic acid (PLA) lattice inner sandwiched together with improved interfaces adhesion. Zareie et al (2022) provided an analysis of the latest advancements in the use of SMA in construction projects, encompassing steel, concrete, and timber structures. Katsiropoulos et al (2020) highlights the importance of SMA in civil structures, namely in improving structural behaviour and dissipating generated energy, especially quake stresses.

Section 2 offers a detailed explanation of the methodology, while Section 3 presents simulation results and discussion. The study concludes in Section 4, providing suggestions for further research.

2. Material sand Methods

2.1 Improved Gradient Graph Convolutional Neural Network (IGGCNN)

This research centres specifically on Young's modulus (YM) as the singular property of interest. Our proposed approach, the Improved Gradient Graph Convolutional Neural Network (IGGCNN), excels in material design, control, and optimization, particularly in identifying optimal solutions that meet specific performance criteria In this work, we provide a machine learning framework for FA, which predicts a material's property from its structure, and ID, which predicts a property from its structure. By a random investigate to find a

representation that mingle a CNN with a Graphical neural network (GNN), a subclass of deep generative models; we are able to achieve inverse design. In this work, we aim to identify a structure possessing the desired attribute by exploring the low-dimensional hidden factors associated with the GNN. The CNN and GNN in this paradigm have distinct responsibilities and taught one another. As a result, requiring the retraining of the intensive GNN is shown in Figure 1.

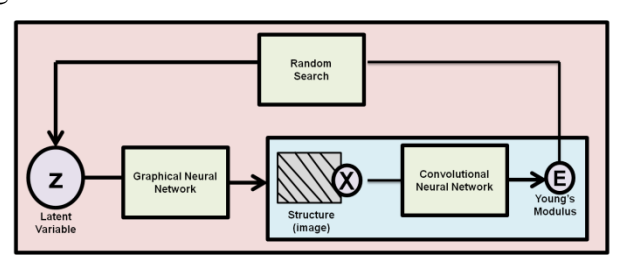


Figure 1. Conceptual diagram of the framework (Source: Author)

2.2. CNN Using FA

Due to its outstanding ability to extract features and recognize patterns, CNN is extensively employed as a deep learning model in various applications, including image recognition and facial expression analysis. It is great relevance to the industrial sector. CNN has numerous layers as a Neural Network (NN). The shared weights of CNN can be used to simplify and modify the neural network's structure. A convolutional network is composed of Fully Connected Layer (FCL) etc. The Conv-pooling module is used to extract features in a consecutive order.

2.3. Convolutional Layer (CL)

A CL also known as a feature extraction layer, it is an N layer used to remove features and mitigate the impact of sound. By applying a sequence of Convolution Kernels (CK) to the input data, CL generates the processed feature map. Every CK in a CL receives data from kernels in the layer below it in a local region. It is a local receptive field associated with distinct geographic regions. Through the establishment of local receptive fields, CKs can extract numerous properties. CL works is described by Equation (1),

$$b_{v}^{u} = \varphi \left(\sum_{o} b_{o}^{v-1} * i_{u}^{v} + d_{u}^{v} \right) \tag{1}$$

The feature map obtained from the u^{th} filter in the i^{th} layer is denoted by b^u_v in this context. b^{v-1}_o explains the nth map of the v-1 layer mentioned. *represent the convolution process. i^v_u is the CK of the u^{th} filter in the v^{th} layer. d^v_u denotes" bias ϕ (.). This value denotes the inauguration utility.

2.3.1 Pooling layer (PL)

PL is also known as feature mapping layers and sample layers. Its major purpose is to remove inferior attribute. The pooling operation's goal is to shrink the network by down sampling the convolutional feature map. Max pooling is a prominent pooling technique in Equation (2)

$$C_{u}^{v} = \max_{(t-1)Y < t < rz} \{b_{u}^{v-1}(t)\} r = 1, 2, \dots$$
 (2)

Where Z is the pooling window size, r is the number of steps moved, $b_u^{v-1}(t)(t)$ represent the cost of the t^{th} neuron in the u^{th} clean" of the v-1 layer, and C_u^v is the attribute chart obtained from the nth filter of the coat.

2.3.2 Fully connected layer (FCL)

The results of the previous PL are transferred into the FCL for further processing of the features. The FCL's primary function is to connect results to the surtax classifier and extract additional features. The FCL is composed several different levels. The operation of an FCL is described by Equation (3),

$$hs^{v+1} = \delta \left(h_{hq}^{v} hq^{u} + D_{hq}^{v} \right) \tag{3}$$

Where h_{hq}^v is "the connection weight matrix," D_{hq}^v is a bias, $\delta(.)$ is the "activation function," and hq^u is "the output of the i^{th} layer".

The cross-entropy function is used to compute a loss function. The irritable-entropy role, which is a valuable "error metric function for pattern recognition," is described in Equation (4).

$$R(G,d) = -\frac{1}{d} \sum_{z=1}^{d} [j^z 1y(f) + (1 - I^z) 1x(1 - f)]$$
(4)

Where b the total number of samples is, j^z is the z^{th} sample's actual value, and f is the classifier's "softmax classifier as shown in Figure 2.

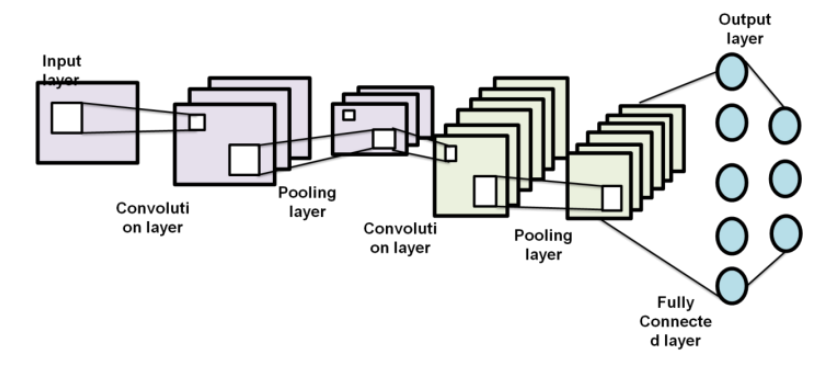


Figure 2. Structure of CNN

(Source: https://www.hindawi.com/journals/cmmm/2021/5557168/)

2.4. GNN Using ID

Graphs are widely working for representing information in diverse factual-world field, and the effectiveness of GNN in managing such data shows great promise. A graph stands out from textual and numerical information due to its unique combination of a feature matrix and an adjacency matrix as shown in Figure 3. Formally, a graph Hwithmnodes is represented by its feature matrixW $\in \mathbb{R}^{m \times c}$ and its adjacency matrixB $\in \{0,1\}^{m \times m}$ we operate under the assumption that every node is equipped with a vector of dimensions, denoted as d, to depict

Nanotechnology Perceptions Vol. 20 No.S3 (2024)

its features. Graph neural networks focus on extracting node description from matrices as part of the learning process. Various GNN variants, including GNN and Graph Attention Networks (GANs), exist despite these matrices' diversity. Utilize a comparable approach to feature learning, where GNNs enhance the features of each node by amalgamating information from its neighbours and integrating it with its own features. To elucidate the process of neighbourhood information aggregation, we employ GNNs as an illustrative example. The definition of GCNs operates is follows in Equation (5):

$$W_{j+1} = f(C^{-\frac{1}{2}} \dot{A} D^{-\frac{1}{2}} W_j X_s), \tag{5}$$

Where $W_j \in \mathbb{R}^{m \times c_j}$ and $W_{j+1} \in \mathbb{R}^{m \times c_{j+1}}$ are the matrices representing input and output features the j th graph complexity layer. In adding $up, \widehat{B} = B + 1$ is old to add self-loops to the adjacency medium, D denotes the slanting bump quantity medium to normalize B. The matrix $W_j \in \mathbb{R}^{c_j \times c_{j+1}}$ is a trainable matrix for layerjand is used to achieve linear feature conversion and $e(\cdot)$ denote a non-linear activation function. The aggregation of hop neighbourhood information is achieved by embankment graph convolution layers. We adopt the diagram difficulty from Equation (5) as our preferred operator for the graph neural network, owing to its outstanding performance.

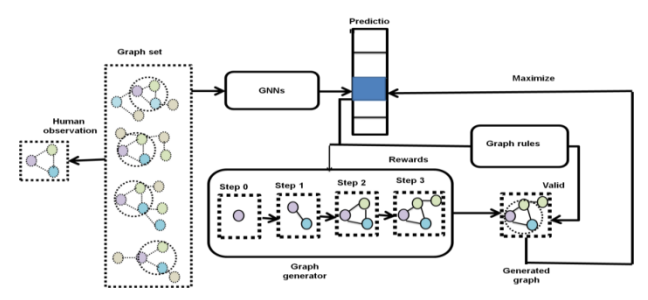


Figure 3. Structure of GNN (Source: Author)

3. Results

This study focuses on Young's modulus as the key parameter. Convolutional neural networks (CNNs) are employed for the forward analysis, while inverse design is accomplished through random searches, resulting in a model that integrates CNNs with Graph Neural Networks (GNNs).

3.1 Forward analysis

We used the data, which included test photos of polymer alloys, to apply the trained CNN. The information is made up of 100 experiment photographs (x) and the matching YM (Y) determined using the RV model (ERVmodel). Figure 4 (a) and (b) presents the findings. We assessed the forecast's performance by comparing the YM predicted by the CNN, Predict, and ERV model using the coefficient of determination, or Q^2 . Relational model evaluation includes the use of measures such as Q^2 . Q^2 is defined as follows: z_j is the ith test label, \overline{z}_j is the machine learning model generates a projected value for the ith test data, while y represents the mean of the test labels in Equation (6).

Nanotechnology Perceptions Vol. 20 No.S3 (2024)

$$Q^{2} = 1 - \frac{\sum_{j}(z_{j} - \widehat{z}_{j})^{2}}{\sum_{j}(z_{j} - \overline{z}_{j})^{2}}$$

$$= 1 - \frac{\sum_{j}(z_{j} - \overline{z}_{j})^{2}}{\sum_{j}(z_{j} - \overline{z}_{j})^{2}}$$

Figure 4(a) RV modulus Young's modulus (b) ERV modulus Young's modulus (Source: Author)

With respect to the experimental photos, we achieved $R^2=0.99$, indicating that the model performs well in terms of prediction. As a result, it was shown that the trained CNN could accurately forecast the YM determined using the RV model. Specifically, the model training under condition D produces a variety of phase parting structure patterns, including gyroid, lamellar, cubic, and disordered formations. Consequently, we made the decision to construct the inverse design framework using the model learned under condition D. It is evident those comparable structures are dispersed in the z plane and that the structure x varies with the hidden variable z. In Figure 5. The tiny structural changes are represented by the z_2 axis, while the z_0 axis depicts the transition from a cubic to a laminated shape .

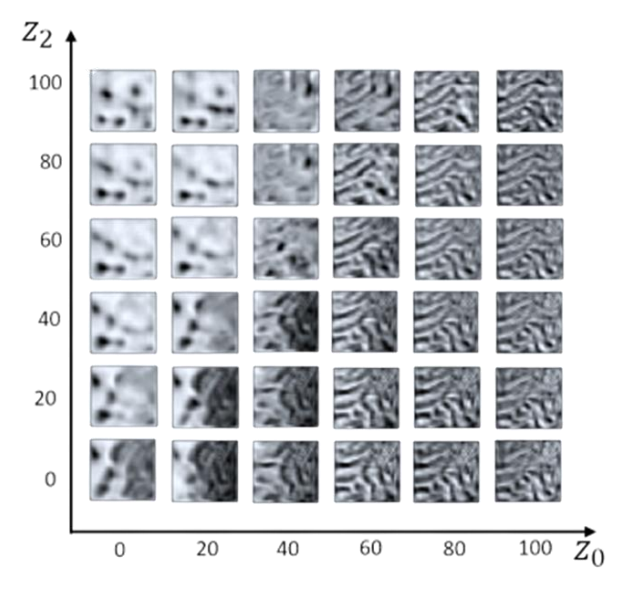


Figure 5Insert Lamellar structure (Source: Author)

3.2 Inverse design

Using the intended Young's modulus E*, we randomly searched the latent patchy z space for the needed construction X* to execute inverse design. A fixed 1000 iterations were used. Since z has four dimensions, this number is suitable for a thorough search. E Become closer and closer to E* while the investigate go on. The outcome of the random search when the intended YM E* was 2000 MPa is shown in Figure 6 (a) and (b). It indicates that the final YM E is really close to E* and that the bent picture x as the WGAN exhibits a polymer alloy possesses a distinctive structure. Moreover, we examined the complete magnitude of the disparity among E* and E and selected 15 targeted Young's moduli E*. E* values were 1780, 1800, 1840, 1880, 1920, 1960, 2000, 2040, 2080, 2120, 2160, 2200, 2240, 2280, and 2320 MPa. There were 1000 iterations total. It is clear that this framework can find constructions with a broad range of intended YM since the average of the complete principles of the 15 discrepancies across E* and E was 0.5 MPa.

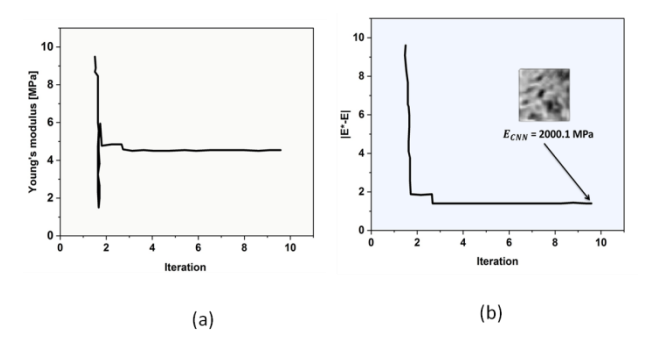


Figure 6(a) Transition of YM E. E approaches E* (b) (Source: Author)

4. Conclusions

The machine learning structure for implementing FA, which predicts a property from a material's structure, and ID, which predicts a construction made of the intended property. We created a support to discuss a polymer alloy's separated phase structural as its composition and YM as its feature, as a specific example. Employing an inverse design approach, the following situations can be handled by the suggested IGGCNN framework: (1) A prerequisite for this task is a dataset containing both the structure and properties derived from experiments or simulations. (2) An identifier capable of encompassing numerous attributes simultaneously. (3) Representation of structures in a three-dimensional context. (4) Supplementary resources are available. It gets used with metals and composite materials that include fibers. More investigation into the best hyper parameter configurations and optimization methods for GGNNs can improve their efficiency. This entails investigating methods such as automated hyper parameter tweaking and Bayesian optimization.

4.1 Limitations of this study

Combining several polymers to create polymer alloys can be difficult, but it can be rewarding when the mix turns out well. Phase separation brought on incompatibility could lower the alloy's overall effectiveness. As opposed to processing individual polymers,

Nanotechnology Perceptions Vol. 20 No.S3 (2024)

manufacturing polymer alloys could be more difficult. For the product to have the desired qualities it is essential to achieve a homogenous mix throughout processing, otherwise, the components can be distributed unevenly.

References

- 1. Daru, L. H. (2019). Hybrid polymer matrix composites: effects of stainless steel and iron oxide particles. University of Johannesburg (South Africa).
- 2. Duarte, I., Krstulović-Opara, L., Dias-de-Oliveira, J., & Vesenjak, M. (2019). Axial crush performance of polymer-aluminium alloy hybrid foam filled tubes. Thin-Walled Structures, 138, 124-136. DOI: 10.1016/j.tws.2019.01.040
- 3. Fakher, S., Khlaifat, A., Hossain, M. E., & Nameer, H. (2021). Rigorous review of electrical submersible pump failure mechanisms and their mitigation measures. Journal of Petroleum Exploration and Production Technology, 11, 3799-3814. DOI: 10.2118/184195-MS
- 4. Feng, Q., & Wang, L. (2022). The effect of polymer composite materials on the comfort of sports and fitness facilities. Journal of Nanomaterials, 2022. DOI: 10.1155/2022/9108458
- 5. Hiraide, K., Oya, Y., Suzuki, M., & Muramatsu, M. (2023). Inverse design of polymer alloys using deep learning based on self-consistent field analysis and finite element analysis. Materials Today Communications, 37, 107233. DOI: 10.1016/j.mtcomm.2023.107233
- 6. Hossain, R., Al Mahmood, A., & Sahajwalla, V. (2021). Facile solution for recycling hazardous flexible plastic-laminated metal packaging waste to produce value-added metal alloys. ACS Sustainable Chemistry & Engineering, 9(50), 16881-16895. DOI: 10.1021/acssuschemeng.1c04368
- 7. Katsiropoulos, C. V., Pappas, P., Koutroumanis, N., Kokkinos, A., & Galiotis, C. (2020). Improving the damping behavior of fiber-reinforced polymer composites with embedded superelastic shape memory alloys (SMA). Smart Materials and Structures, 29(2), 025006. DOI: 10.1088/1361-665X/ab6026
- 8. Mann, A., & Kalidindi, S. R. (2022). Development of a robust CNN model for capturing microstructure-property linkages and building property closures supporting material design. Frontiers in materials, 9, 851085 DOI: 10.3389/fmats.2022.851085
- 9. Meng, X., Huang, Y., Cao, J., Shen, J., & dos Santos, J. F. (2021). Recent progress on control strategies for inherent issues in friction stir welding. Progress in Materials Science, 115, 100706. DOI: 10.1016/j.pmatsci.2020.100706
- Neamţu, B. V., Irimie, A., Popa, F., Gabor, M. S., Marinca, T. F., & Chicinaş, I. (2020). Soft magnetic composites based on oriented short Fe fibres coated with polymer. Journal of Alloys and Compounds, 840, 155731. DOI: 10.1016/j.jallcom.2020.155731
- 11. Saeed, N., King, N., Said, Z., & Omar, M. A. (2019). Automatic defects detection in CFRP thermograms, using convolutional neural networks and transfer learning. Infrared Physics & Technology, 102, 103048. DOI: 10.1016/j.infrared.2019.103048
- 12. Shaikh, N. S., Ubale, S. B., Mane, V. J., Shaikh, J. S., Lokhande, V. C., Praserthdam, S., ... & Kanjanaboos, P. (2022). Novel electrodes for supercapacitor: Conducting polymers, metal oxides, chalcogenides, carbides, nitrides, MXenes, and their composites with graphene. Journal of Alloys and Compounds, 893, 161998. DOI: 10.1016/j.jallcom.2021.161998
- 13. Shajkofci, A., & Liebling, M. (2020). Spatially-variant CNN-based point spread function estimation for blind deconvolution and depth estimation in optical microscopy. IEEE Transactions on Image Processing, 29, 5848-5861. DOI: 10.1109/TIP.2020.2986880
- 14. Tabish, A., Varghese, A. M., Wahab, M. A., & Karanikolos, G. N. (2020). Perovskites in the energy grid and CO2 conversion: Current context and future directions. Catalysts, 10(1), 95.

- DOI: 10.3390/catal10010095
- Wang, T. C., Zhu, J. Y., Hiroaki, E., Chandraker, M., Efros, A. A., & Ramamoorthi, R. (2016).
 A 4D light-field dataset and CNN architectures for material recognition. In Computer Vision–ECCV 2016: 14th European Conference, Amsterdam, The Netherlands, October 11-14, 2016, Proceedings, Part III 14 (pp. 121-138). Springer International Publishing. DOI: 10.1007/978-3-319-46487-9 8
- Yamanaka, J., Kuwashima, S., & Kurita, T. (2017). Fast and accurate image super resolution by deep CNN with skip connection and network in network. In Neural Information Processing: 24th International Conference, ICONIP 2017, Guangzhou, China, November 14-18, 2017, Proceedings, Part II 24 (pp. 217-225). Springer International Publishing. DOI: 10.1007/978-3-319-70096-0_23
- 17. Yan, C., Feng, X., Wick, C., Peters, A., & Li, G. (2021). Machine learning assisted discovery of new thermoset shape memory polymers based on a small training dataset. Polymer, 214, 123351. DOI: 10.1016/j.polymer.2020.123351
- 18. Zareie, S., Issa, A. S., Seethaler, R. J., & Zabihollah, A. (2020, October). Recent advances in the applications of shape memory alloys in civil infrastructures: A review. In Structures (Vol. 27, pp. 1535-1550). Elsevier. DOI:10.1016/j.istruc.2020.05.058
- 19. Zarrintaj, P., Saeb, M. R., Jafari, S. H., & Mozafari, M. (2020). Application of compatibilized polymer blends in biomedical fields. In Compatibilization of Polymer Blends (pp. 511-537). DOI: 10.1016/B978-0-12-816006-0.00018-9
- 20. Zhou, X., Li, J., Qu, C., Bu, W., Liu, Z., Fan, Y., & Bao, G. (2022). Bending behavior of hybrid sandwich composite structures containing 3D printed PLA lattice cores and magnesium alloy face sheets. The Journal of Adhesion, 98(11), 1713-1731. DOI: 10.1080/00218464.2021.1939015